An improved FEM-DEM coupling simulation for granular-media-based thin-wall elbow tube push-bending process

Hai Liu*, Guang-Hui Ma, Zhe Geng

Department of Precision Manufacturing Engineering, Suzhou Vocational Institute of Industrial Technology, 1 Zhineng Avenue, Suzhou 215104, P.R. China.

Abstract:
The granular-media-based push-bending process has been developed to manufacture thin-wall elbow tube with t/D≤0.01 (the ratio of wall thickness to outer diameter) and R/D≤1.5 (the ratio of bending radius to outer diameter). In the process, a tubular blank is filled with granular media and then pushed into a die to form an elbow shape. To investigate the process, a FEM-DEM coupling model has been developed, in which FEM is used to simulate bending deformation of tubular blank, and DEM is used to calculate contact forces between spherical particles in granular media. In this work, an improved numerical formulation is proposed in order to reach mechanical equilibrium quickly and accelerate the convergence of DEM simulation, when the new contacts are no longer created and the old contacts are no longer deleted in granular media. Using the proposed numerical formulation, the improved FEM-DEM coupling simulation for granular-media-based thin-wall elbow tube push-bending process is less time-consuming than before under the same simulation condition.

Keyword: elbow tube; granular-media-based; push bending; energetic formulation; FEM-DEM coupling

1 Introduction

The thin-wall elbow tubes with t/D≤0.01 and R/D≤1.5 (where t is wall thickness, D is outer diameter, and R is bending radius) are widely used in rocket engine pipelines [1-3]. In the bending process of elbow tube with quite small t/D and R/D, the forming defects such as wrinkling and fracture is difficult to be avoided, and the dimensional precision is difficult to satisfy the requirements due to the springback and cross-sectional ovalization. Push-bending process is demonstrated to be applicable for manufacturing elbow tubes with small R/D [4-5]. The recently developed granular-media-based push-bending process can be used to manufacture the thin-wall elbow tube with t/D≤0.01 and R/D≤1.5 as required [6]. The granular-media-based thin-wall elbow push-bending process involves filling a tube with spherical granular media and pushing the tube into a die to bend a tubular blank into an elbow shape. The spherical granular media introduced as filler has great potential for its flexibility [7], resistance to high forming temperature [8-9], and characteristics of pressure-transmission [10-

* E-mail address: hliu@alum.imr.ac.cn

11]. In addition, the spherical granular media is controllable and predictable because of its regular shape.

To investigate the granular-media-based thin-wall elbow push-bending process, a 3D FEM-DEM coupling model is developed [12]. In the coupling model, FEM is used to simulate bending deformation of tubular blank (continuum), and DEM is used to calculate contact forces between spherical particles in granular media (discrete media). DEM is a dynamic method, and damping is applied to the equations of motion in order to absorb vibration energy and reach mechanical equilibrium. The biggest time overhead in the coupling model is absorbing vibration energy in DEM simulation to reach mechanical equilibrium. To accelerate the convergence of DEM simulation, a static energetic method is proposed in the present paper.

Generally in the earlier stage of DEM simulation, some new contacts between pairs of particles are detected and created, and some old contacts are broken and deleted. But in the later stage of DEM simulation, the new contacts are no longer detected and created, the old contacts are no longer broken and deleted, and a static energetic formulation can be used to determine mechanical equilibrium.

2 Mechanical model

The granular-media-based push-bending process is illustrated in Fig.1. A tubular blank with predetermined dimensions and filled with granular media is inserted into the die and then deformed according to the shape of the die. The tubular blank is bended under the forming force of punch, constraint force of die, and interaction of granular filler. The forming force of punch and constraint force of die is simulated with FEM. The contact forces between neighbor particles in granular media is simulated with DEM.

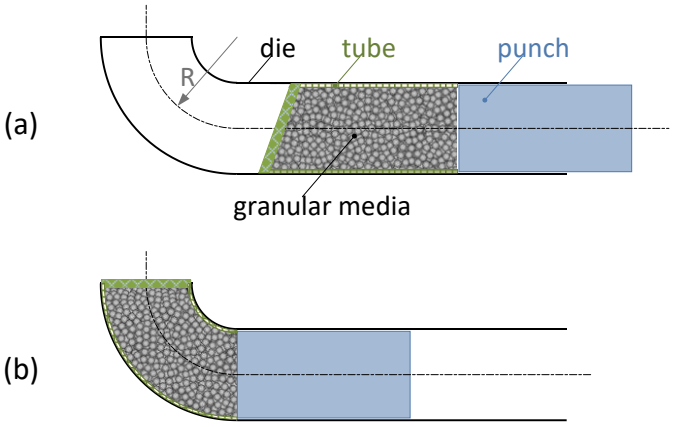

Fig. 1 The illustration of the granular-media-based thin-wall elbow push-bending process: (a) before bending, (b) bending.

2.1 Kinematics

In the DEM simulation, when the new contacts are no longer created and the old contacts are no longer deleted in granular media, the positions of the spherical particles are collected in the 3×1 column matrixes:

$$\mathbf{x}_i = [x_{i1} \quad x_{i2} \quad x_{i3}]^{\mathrm{T}} \tag{2.1}$$

where x_{il} denotes the *l-th* position component of the *i-th* particle. The spherical particles in the granular media are labeled by the indexes *i*=1, 2, 3…*N*.

In the same way, the centroid displacements and the rotation components of particles are collected in the 3×1 column matrixes:

$$\begin{aligned} \mathbf{v}_i &= [v_{i1} \quad v_{i2} \quad v_{i3}]^{\mathrm{T}} \\ \mathbf{w}_i &= [w_{i1} \quad w_{i2} \quad w_{i3}]^{\mathrm{T}} \end{aligned} \tag{2.2}$$

where v_{il} denotes the *l-th* displacement component of the *i-th* particle, and w_{il} denotes the *l-th* rotation component of the *i-th* particle.

The contact k_c formed by the particle *i* and the particle *j*, in shown in Fig.2.

Assuming that elastic deformations are localized in very small neighborhoods of the contact points, so that, the relative displacement between the rigid part of the two particles near the contact point $\mathbf{x}^{(k_c)}$ is:

$$\Delta\boldsymbol{\delta}_{k_c} = \left(\mathbf{v}_j - \mathbf{v}_i\right) + R\tilde{\mathbf{n}}_{k_c}\left(\mathbf{w}_j + \mathbf{w}_i\right) \tag{2.3}$$

where *R* denotes the particle radius, $\tilde{\mathbf{n}}_{k_c}$ denotes the antisymmetric matrix formed by the components of the unit normal vector $\mathbf{n}_{k_c}$.

$$\tilde{\mathbf{n}}_{k_c} = \begin{bmatrix} 0 & n_{k_c3} & -n_{k_c2} \\ -n_{k_c3} & 0 & n_{k_c1} \\ n_{k_c2} & -n_{k_c1} & 0 \end{bmatrix} \tag{2.4}$$

If the contact point $\mathbf{x}^{(k_c)}$ is formed by the particles *i* and *j*, we have:

$$\mathbf{n}_{k_c} = \frac{(\mathbf{x}_j - \mathbf{x}_i)}{|\mathbf{x}_j - \mathbf{x}_i|} \qquad k_c = 1,2,\dots,M_c \tag{2.5}$$

If the contact point $\mathbf{x}^{(k_c)}$ is formed by the particles *i* and the boundary wall, we have:

$$\mathbf{n}_{k_c} = \frac{(\mathbf{x}_{Bk_c} - \mathbf{x}_i)}{|\mathbf{x}_{Bk_c} - \mathbf{x}_i|} \qquad k_c = 1,2,\dots,M_b \tag{2.6}$$

where $\mathbf{x}_{Bk_c}$ denotes the contact point of index k_c between the particle *i* and the boundary wall.

Assuming that the relative displacement $\Delta\boldsymbol{\delta}_{k_c}$ is small, the change of distance between the two neighbor particles' centers can be determined as the normal component of their relative displacement, which is set equal to an incremental normal overlap:

$$\begin{aligned} &-\Delta\alpha_{k_c} = \mathbf{n}_{k_c}^{\mathrm{T}}\Delta\boldsymbol{\delta}_{k_c} = \mathbf{n}_{k_c}^{\mathrm{T}}\left[\left(\mathbf{v}_j - \mathbf{v}_i\right) + R\tilde{\mathbf{n}}_{k_c}\left(\mathbf{w}_j + \mathbf{w}_i\right)\right] = \mathbf{n}_{k_c}^{\mathrm{T}}\left(\mathbf{v}_j - \mathbf{v}_i\right) \\ &\Delta\alpha_{k_c} = -\alpha_{k_c}, \ if \ \ \Delta\alpha_{k_c} < -\alpha_{k_c} \\ &k_c = 1,2,\dots,M_c \end{aligned} \tag{2.7}$$

where $\Delta\alpha_{k_c}$ is positive if the distance between the two centers decreases, while $\Delta\alpha_{k_c}$ is negative if the distance between the two centers increases. When $\Delta\alpha_{k_c}$ is

negative, $\Delta\alpha_{k_c}$ can not be smaller than the initial normal overlap α_{k_c}. M_c is the total number of contacts in the granular media.

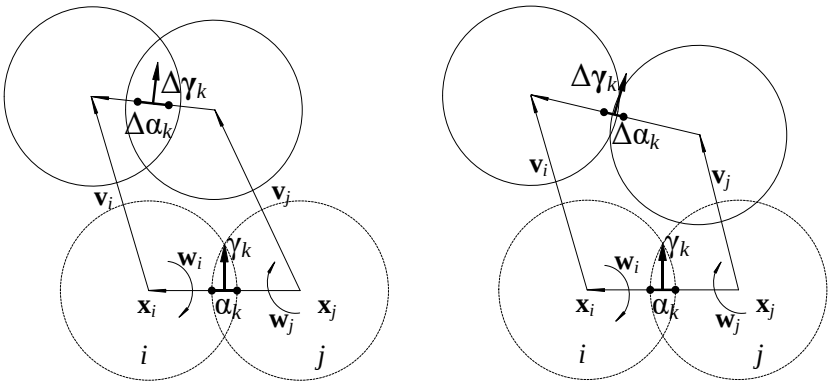

Fig.2 Relation between normal overlap and displacements of a pair of spherical particles in contact. The dashed circles denote the initial positions and the solid circles denote the positions after loading.

In a similar way, the incremental tangential relative displacement due to the elastic deformations of particles can be written as:

$$\begin{aligned}\Delta\boldsymbol{\gamma}_{k_c} &= \left(\mathbf{I}-\mathbf{n}_{k_c}\mathbf{n}_{k_c}^{\mathrm{T}}\right)\Delta\boldsymbol{\delta}_{k_c}\\ &= \left(\mathbf{I}-\mathbf{n}_{k_c}\mathbf{n}_{k_c}^{\mathrm{T}}\right)\left[\left(\mathbf{v}_j-\mathbf{v}_i\right)+R\tilde{\mathbf{n}}_{k_c}\left(\mathbf{w}_j+\mathbf{w}_i\right)\right]\\ &= \left(\mathbf{I}-\mathbf{n}_{k_c}\mathbf{n}_{k_c}^{\mathrm{T}}\right)\left(\mathbf{v}_j-\mathbf{v}_i\right)+R\tilde{\mathbf{n}}_{k_c}\left(\mathbf{w}_j+\mathbf{w}_i\right) \qquad k_c=1,2,\ldots,M_c\end{aligned} \tag{2.8}$$

Further, eq.(2.8) can be rewritten as:

$$\Delta\boldsymbol{\gamma}_{k_c}=\tilde{\boldsymbol{\gamma}}_{k_c}\Delta\alpha_{k_c} \tag{2.9}$$

where $\tilde{\boldsymbol{\gamma}}_{k_c}$ denotes the slope vector with respect the unit normal vector $\mathbf{n}_{k_c}$ of the contact elastic relative displacement $\Delta\boldsymbol{\delta}_{k_c}$.

In the same way, when the particle *i* is in contact with the boundary wall, we have:

$$\begin{aligned}-\Delta\alpha_{k_c} &= \mathbf{n}_{k_c}^{\mathrm{T}}\left(\bar{\mathbf{v}}_{\mathrm{B}k_c}-\mathbf{v}_i\right)\\ \Delta\boldsymbol{\gamma}_{k_c} &= \left(\mathbf{I}-\mathbf{n}_{k_c}\mathbf{n}_{k_c}^{\mathrm{T}}\right)\left[\bar{\mathbf{v}}_{\mathrm{B}k_c}-\mathbf{v}_i+R\tilde{\mathbf{n}}_{k_c}\mathbf{w}_i\right]=\tilde{\boldsymbol{\gamma}}_{k_c}\Delta\alpha_{k_c} \qquad k_c=1,2,\ldots,M_b\end{aligned} \tag{2.10}$$

The unknown displacements and rotations of the particles are collected in the 6*N*×1column matrix **U**:

$$\begin{aligned}\mathbf{U}^{\mathrm{T}} &= [\mathbf{V}^{\mathrm{T}} \quad \mathbf{W}^{\mathrm{T}}]\\ \mathbf{V}^{\mathrm{T}} &= [v_{11}\ v_{12}\ v_{13}\ \ldots\ v_{i1}\ v_{i2}\ v_{i3}\ \ldots\ v_{N1}\ v_{N2}\ v_{N3}]^{\mathrm{T}}\\ \mathbf{W}^{\mathrm{T}} &= [w_{11}\ w_{12}\ w_{13}\ \ldots\ w_{i1}\ w_{i2}\ w_{i3}\ \ldots\ w_{N1}\ w_{N2}\ w_{N3}]^{\mathrm{T}}\end{aligned} \tag{2.11}$$

The incremental normal overlaps of contacts between spherical particles are collected in the M_c×1 column matrixes $\Delta\boldsymbol{\alpha}_{\mathrm{C}}$. The incremental tangential relative displacements are collected in the 3M_c×1 column matrixes $\Delta\boldsymbol{\gamma}_{\mathrm{C}}$. In the same way, the incremental relative displacements of the contacts between spherical particles and the boundary wall are collected in the M_b×1 column matrixes $\Delta\boldsymbol{\alpha}_{\mathrm{B}}$ and in the 3M_b×1 column matrixes $\Delta\boldsymbol{\gamma}_{\mathrm{B}}$. Then, the equations from (2.3) to (2.10) can be summarized as:

$$\begin{cases} \Delta\boldsymbol{\delta} = \begin{bmatrix} -\Delta\boldsymbol{\alpha} \\ \Delta\boldsymbol{\gamma} \end{bmatrix} = \mathbf{A}^{\mathrm{T}}\Delta\mathbf{U} \\ \Delta\boldsymbol{\gamma} = \tilde{Y}\Delta\boldsymbol{\alpha} \\ \left[\tilde{Y}\right] = \left[\tilde{\boldsymbol{\gamma}}_1 \quad \tilde{\boldsymbol{\gamma}}_2 \quad \cdots \quad \cdots \quad \tilde{\boldsymbol{\gamma}}_{M_c+M_b}\right] \end{cases} \tag{2.12}$$

where $\mathbf{A}^{\mathrm{T}} = \begin{bmatrix} \mathbf{n}^{\mathrm{T}} & \mathbf{0} \\ (\mathbf{I} - \mathbf{n}\mathbf{n}^{\mathrm{T}}) & \mathrm{R}\tilde{\boldsymbol{n}} \end{bmatrix}$ is a (4M_c+4M_b)×6N matrix composed by unit normal vectors $\mathbf{n}_{k_c}$.

2.2 Statics

Due to the deformations of particles, the compressive normal forces and tangential forces are developed. The equilibrium equations of the particles can be written as:

$$\begin{aligned} &\mathbf{A}\mathbf{F} = \mathbf{A}_{\mathrm{C}}\mathbf{F}_{\mathrm{C}} + \mathbf{A}_{\mathrm{B}}\mathbf{F}_{\mathrm{B}} = \mathbf{T} \\ &\mathbf{F}_{\mathrm{C}}^{\mathrm{T}} = \begin{bmatrix} \mathbf{N}_{\mathrm{C}}^{\mathrm{T}} & \mathbf{V}_{\mathrm{C}}^{\mathrm{T}} \end{bmatrix} \\ &\mathbf{F}_{\mathrm{B}}^{\mathrm{T}} = \begin{bmatrix} \mathbf{N}_{\mathrm{B}}^{\mathrm{T}} & \mathbf{V}_{\mathrm{B}}^{\mathrm{T}} \end{bmatrix} \end{aligned} \tag{2.13}$$

where $\mathbf{N}_{\mathrm{B}}$ is the M_b×1 column matrix of the normal compressive contact forces and $\mathbf{V}_{\mathrm{B}}$ is the 3M_b×1 column matrix of the tangential contact forces exerted on the boundary wall; $\mathbf{N}_{\mathrm{C}}$ is the M_c×1 column matrix of the normal compressive contact forces exerted in the contacts between spherical particles and $\mathbf{V}_{\mathrm{C}}$ is the 3M_c×1 column matrix of the tangential contact forces; **T** is the 6N×1 column matrix of the external forces (such as gravity, boundary forces).

2.3 Contact-Stiffness Model

After the equilibrium and kinematic relations are established, a contact force-relative displacement law must be introduced. The DEM simulation in this work is performed using PFC^{3D} solver. PFC^{3D} provides two stiffness models: a linear model and a simplified Hertz-Mindlin model. In the linear model, the forces and relative displacements are linearly related by the constant contact stiffness. Here, the linear contact model is adopted, which can be written as:

$$\begin{cases} N_{k_c} = k^n \alpha_{k_c} \\ \Delta\mathbf{V}_{k_c} = k^s \Delta\boldsymbol{\gamma}_{k_c} \end{cases} \tag{2.14}$$

where k^n and k^s are the normal and shear-contact stiffnesses.

The above relation (2.14) can be summarized in the form of matrix as follows:

$$\begin{cases} \mathbf{N} = \mathbf{K}^{\mathrm{n}}\boldsymbol{\alpha} \\ \Delta\mathbf{V} = \mathbf{K}^{\mathrm{s}}\Delta\boldsymbol{\gamma} \end{cases} \tag{2.15}$$

2.4 Incremental work

We assume that in a given equilibrium state the elastic displacement vector is $\overline{\boldsymbol{\delta}} = (\overline{\boldsymbol{\alpha}}, \overline{\boldsymbol{\gamma}})$ and that a small incremental elastic displacement vector $\Delta\boldsymbol{\delta} = (\Delta\boldsymbol{\alpha}, \Delta\boldsymbol{\gamma})$ is further applied. Then the incremental work done by the contact forces can be written as:

$$\int_{\overline{\boldsymbol{\delta}}}^{\overline{\boldsymbol{\delta}}+\Delta\boldsymbol{\delta}} \mathbf{F}(\boldsymbol{\delta})^{\mathrm{T}} d\boldsymbol{\delta} = \overline{\mathbf{F}}^{\mathrm{T}}\Delta\boldsymbol{\delta} + \frac{1}{2}\Delta\mathbf{F}^{\mathrm{T}}\Delta\boldsymbol{\delta} \tag{2.16}$$

In the same way, the incremental work done by the external forces can be written as:

$$\int_{\bar{\mathbf{U}}}^{\bar{\mathbf{U}}+\Delta\mathbf{U}} \mathbf{T}^{\mathrm{T}} d\mathbf{U} = \bar{\mathbf{T}}^{\mathrm{T}}\Delta\mathbf{U} + \frac{1}{2}\Delta\mathbf{T}^{\mathrm{T}}\Delta\mathbf{U} \tag{2.17}$$

In view of (2.12) and (2.13), the equation (2.17) can be rewritten as:

$$\int_{\bar{\mathbf{U}}}^{\bar{\mathbf{U}}+\Delta\mathbf{U}} \mathbf{T}^{\mathrm{T}} d\mathbf{U} = \bar{\mathbf{F}}^{\mathrm{T}}\mathbf{A}^{\boldsymbol{T}}\Delta\mathbf{U} + \frac{1}{2}\Delta\mathbf{T}^{\mathrm{T}}\Delta\mathbf{U} = \bar{\mathbf{F}}^{\mathrm{T}}\Delta\boldsymbol{\delta} + \frac{1}{2}\Delta\mathbf{T}^{\mathrm{T}}\Delta\mathbf{U} \tag{2.18}$$

An incremental total energy is defined as:

$$\Psi(\Delta\mathbf{U}) = \int_{\bar{\boldsymbol{\delta}}}^{\bar{\boldsymbol{\delta}}+\Delta\boldsymbol{\delta}} \mathbf{F}(\boldsymbol{\delta})^{\mathrm{T}} d\boldsymbol{\delta} - \int_{\bar{\mathbf{U}}}^{\bar{\mathbf{U}}+\Delta\mathbf{U}} \mathbf{T}^{\mathrm{T}} d\mathbf{U} = \frac{1}{2}\Delta\mathbf{F}^{\mathrm{T}}\Delta\boldsymbol{\delta} - \frac{1}{2}\Delta\mathbf{T}^{\mathrm{T}}\Delta\mathbf{U} \tag{2.19}$$

2.5 Minimum principle for incremental total energy

In the following, we will assign a superscript * both to any kinematically admissible system of incremental displacements and to any mechanical quantity associated to it by means of eq. from (2.12) to (2.19). Then we have:

$$\Psi(\Delta\mathbf{U}^*) - \Psi(\Delta\mathbf{U}) = \frac{1}{2}\left(\Delta\mathbf{F}^{*\mathrm{T}}\Delta\boldsymbol{\delta}^* - \Delta\mathbf{F}^{\mathrm{T}}\Delta\boldsymbol{\delta}^*\right) + \frac{1}{2}\Delta\mathbf{T}^{\mathrm{T}}(\Delta\mathbf{U} - \Delta\mathbf{U}^*) \tag{2.20}$$

In view of (2.12) and (2.13), the equation (2.20) can be rewritten as:

$$\begin{aligned}
&\Psi(\Delta\mathbf{U}^*) - \Psi(\Delta\mathbf{U}) = \frac{1}{2}\left(\Delta\mathbf{F}^{*\mathrm{T}}\Delta\boldsymbol{\delta}^* - \Delta\mathbf{F}^{\mathrm{T}}\Delta\boldsymbol{\delta}^*\right) + \frac{1}{2}\Delta\mathbf{F}^{\mathrm{T}}\mathbf{A}^{\boldsymbol{T}}(\Delta\mathbf{U} - \Delta\mathbf{U}^*) \\
&= \frac{1}{2}\left(\Delta\mathbf{F}^{*\mathrm{T}} - \Delta\mathbf{F}^{\mathrm{T}}\right)\Delta\boldsymbol{\delta}^* + \frac{1}{2}\Delta\mathbf{F}^{\mathrm{T}}(\Delta\boldsymbol{\delta} - \Delta\boldsymbol{\delta}^*) \\
&= \frac{1}{2}(\Delta\boldsymbol{\delta}^* - \Delta\boldsymbol{\delta})^{\boldsymbol{T}}\mathbf{K}(\Delta\boldsymbol{\delta}^* - \Delta\boldsymbol{\delta})
\end{aligned} \tag{2.21}$$

where $\mathbf{K} = \begin{bmatrix} \mathrm{K}^{\mathrm{n}} & \mathbf{0} \\ \mathbf{0} & \mathrm{K}^{\mathrm{s}} \end{bmatrix}$ is the stiffness matrix, which is diagonal and definite positive. it can be noted that, $\Psi(\Delta\mathbf{U}^*) - \Psi(\Delta\mathbf{U})$ is always positive. So it can be concluded that, The incremental total energy $\Psi(\Delta\mathbf{U}^*)$ attains its minimum if the kinematically admissible system of incremental displacements is such to satisfy the equilibrium equations (2.13).

3 Numerical model

The minimum principle for incremental total energy $\Psi(\Delta\mathbf{U}^*)$ proposed in the section 2, can be used to accelerate the convergence of DEM simulation. The numerical form of the minimum principle can be written as:

$$\begin{aligned}
&\min \quad \frac{1}{2}\Delta\mathbf{U}^{*\mathrm{T}} \cdot \mathbf{A}\mathbf{K}\mathbf{A}^{\mathrm{T}} \cdot \Delta\mathbf{U}^* - \frac{1}{2}\Delta\mathbf{T}^{\mathrm{T}}\Delta\mathbf{U}^* \\
&\text{s.t.} \begin{cases} \mathbf{K}\mathbf{A}_{\boldsymbol{B}}^{\boldsymbol{T}}\Delta\mathbf{U}^* = \Delta\mathbf{F}_{\boldsymbol{B}} \\ \mathbf{A}^{\mathrm{T}} = \begin{bmatrix} \mathbf{n}^{\mathrm{T}} & \mathbf{0} \\ (\mathbf{I} - \mathbf{n}\mathbf{n}^{\mathrm{T}}) & \mathrm{R}\tilde{\boldsymbol{n}} \end{bmatrix} \\ \mathbf{K} = \begin{bmatrix} \mathrm{K}^{\mathrm{n}} & \mathbf{0} \\ \mathbf{0} & \mathrm{K}^{\mathrm{s}} \end{bmatrix} \end{cases}
\end{aligned} \tag{3.1}$$

where $\mathbf{F}_{\mathrm{B}}$ denotes the contact forces exerted on the boundary wall, which is equal to the external boundary force.

In this work, the movement and interaction of spherical particles is modeled by PFC^{3D}. In the later stage of PFC^{3D} modeling, when the new contacts are no longer detected and created, and the old contacts are no longer broken and deleted, the equation (3.1) is introduced in order to reach mechanical equilibrium quickly. The improved DEM formulation is shown in Fig.3.

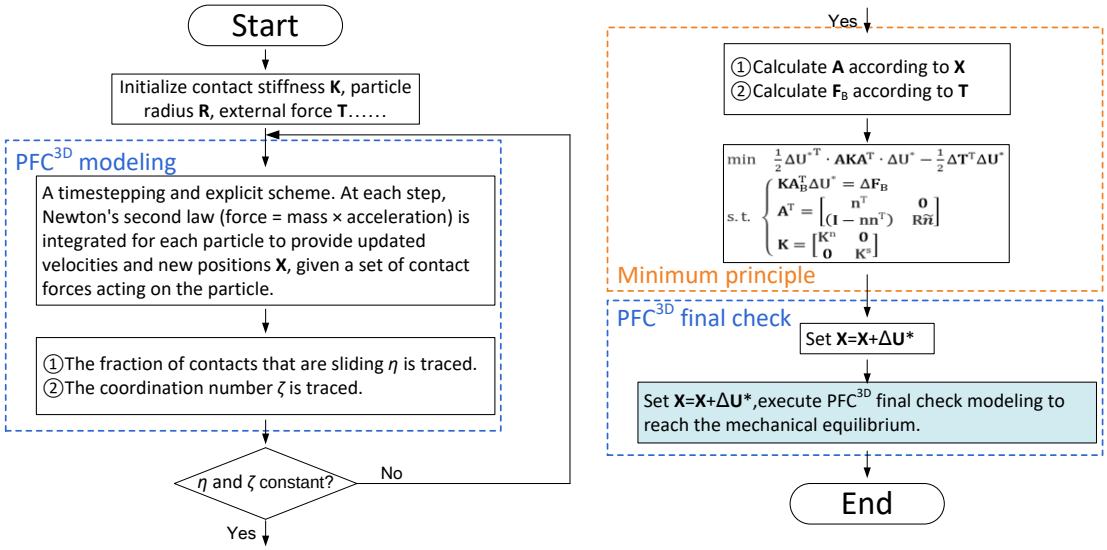

Fig.3 The improved DEM formulation based on the minimum principle for incremental total energy

In order to require modest sizes of computer memory, considering the incremental work is mainly done by the normal contact forces, the numerical srategy can be rewritten as:

$$\begin{aligned} &\min \quad \frac{1}{2}\Delta\mathbf{V}^{*\mathrm{T}}\cdot\mathbf{A}\mathbf{K}^{\mathrm{n}}\mathbf{A}^{\mathrm{T}}\cdot\Delta\mathbf{V}^{*}-\frac{1}{2}\Delta\mathbf{T}^{\mathrm{T}}\Delta\mathbf{V}^{*} \\ &\text{s.t.}\ \begin{cases}\mathbf{A}^{\mathrm{T}}=\mathbf{n}^{\mathrm{T}}\\ \mathrm{K}^{\mathrm{n}}\mathbf{A}_{\boldsymbol{B}}^{\boldsymbol{T}}\Delta\mathbf{V}^{*}=\Delta\mathbf{F}_{\boldsymbol{B}}\end{cases} \end{aligned} \tag{3.2}$$

The equation (3.2) is also introduced into the improved DEM formulation shown in Fig.3 to observe the computational efficiency.

4 The examination of the numerical model

The improved DEM formulation is examined numerically using the 3D FEM-DEM coupling model reported by Liu et al. [12].

In the FEM model, an elbow tube of stainless steel (1Cr18Ni9Ti) with wall thickness t=0.3mm, outer diameter D=30mm, bending radius R=90mm, is formed. The FEM model of ABAQUS [13] shown in Fig.4(a), considers nonlinear geometry through a large-strain description of elbow tube, and material is considered both elastic and elastic-plastic (1Cr18Ni9Ti stainless steel). The FEM model is three-dimensional, and four-node reduced-integration shell elements (S4R) are employed for modeling of the thin-wall elbow tube. Contact forces between particles and tube are imposed on the four nodes nearby the particle-tube contact points in the form of concentrated force. Regarding the number of elements in the longitudinal direction, at least 5 elements

per particle size are employed in the tube. Friction coefficient between die and tube is set 0.05.

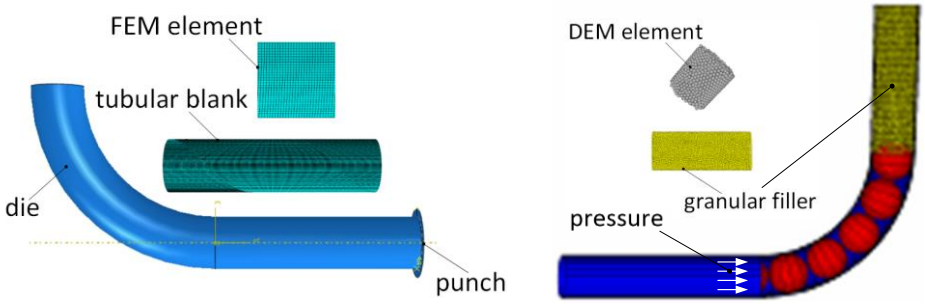

(a) (b)

Fig.4 The FEM model of the elbow tube push-bending

It is shown in Fig.4(b) that, the cast iron granular media with particle diameter 1.58mm is modeled as filler by DEM. Wall boundary is created according to the tube shape determined in FEM. The linear model with constant stiffness is employed to model the particle-wall and inter-particle contacts. The friction coefficients of both particle-wall and inter-particle are set 0.05.

In the FEM-DEM coupling program, at the *i*th increment, the shape of tube is calculated in FEM under the force boundary conditions (contact forces between particles and tube) determined at the (*i-1)*th increment in DEM. The contact forces distribution in granular media is calculated in DEM under the displacement boundary conditions (tube shape) determined at the (*i-1)*th increment in FEM.

The time-consuming results of the different FEM-DEM coupling models with no minimum principle, with the equation (3.1) and with the equation (3.2) under the same simulation condition, are listed in Table 1.

Table 1. The time-consuming results of the different FEM-DEM coupling models

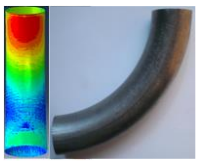	Not using the minimum principle	Using the equation (3.1)	Using the equation (3.2)
Time consuming(hour)	≈210	≈170	≈120

It is shown in Table 1 that, the improved FEM-DEM coupling simulation using the minimum principle eq.(3.1) or eq.(3.2) is less time-consuming than the previous coupling model.

5 Conclusions

Considering the new contacts are no longer created and the old contacts are no longer deleted in the later stage of DEM simulation, an improved numerical formulation is proposed in order to reach mechanical equilibrium quickly and accelerate the convergence of DEM simulation. The improved numerical formulation

is based on the minimum principle for incremental total energy in granular media. The improved DEM formulation is examined numerically using the 3D FEM-DEM coupling model of the granular-media-based thin-wall elbow tube push-bending process. It is demonstrated that the improved FEM-DEM coupling model is less time-consuming than the previous under the same simulation condition.

Funding Information

The present work is funded by the Scientific Research Foundation of SIIT (2022kyqd001), Natural Science Research General Project of Universities in Jiangsu Province (no.21KJB430006).

References

[1] H. Yang, H. Li, Z.Y. Zhang, et al. Advances and trends on tube bending forming technologies. Chinese J. Aeronaut. 2012, 25: 1-12

[2] B.G. Teng, L. Hu, G. Liu, S.J. Yuan. Wrinkling behavior of hydro bending of carbon steel Al alloy bilayered tubes. Trans. Nonferrous Met. Soc. China. 2012, 22:560−565

[3] H. Yang, H. Li, Z. Zhang, M. Zhan, J. Liu, G. Li. Advances and trends on tube bending forming technologies. J. Plast. Eng. 2012, 8: 83–85

[4] Y. Zeng, Z. Li. Experimental research on the tube push-bending process. Journal of Materials Processing Technology. 2002, 122(2-3): 237-240

[5] Oh I Y, Han S W, Woo Y Y, et al. Tubular blank design to fabricate an elbow tube by a push-bending process. Journal of Materials Processing Technology. 2018, 260:112-122

[6] H. Liu, S.H. Zhang, Y.P. Ding, et al. A simplified formulation for predicting wrinkling of thin-wall elbow tube in granular media–based push-bending process. International Journal of Advanced Manufacturing Technology. 2021, 115: 541-549

[7] B. Du, C.C. Zhao, G.J. Dong, et al. FEM-DEM coupling analysis for solid granule medium forming new technology. J. Mater. Process. Technol. 2017, 249: 108-117

[8] H. Chen, A. Güner, N.B. Khalifa, A.E. Tekkaya. Granular media-based tube press hardening. J. Mater. Process. Technol. 2016, 228: 145–159

[9] H. Chen, S. Hess, J. Haeberle, S. Pitikaris, P. Born, A. Güner, M. Sperl, A.E. Tekkaya. Enhanced granular medium-based tube and hollow profile press hardening. CIRP Ann.-Manuf. Technol. 2016, 65: 273–276

[10] G.J. Dong, C.C. Zhao, Y.X. Peng, Y. Li. Hot granules medium pressure forming process of AA7075 conical parts. Chin. J. Mech. Eng. 2015, 28: 580–591

[11] G.J. Dong, J. Bi, B. Du, C.C. Zhao. Research on AA6061 tubular components prepared by combined technology of heat treatment and internal high pressure forming. J. Mater. Process. Technol. 2017, 242: 126–138

[12] H. Liu, S.H. Zhang, H.W. Song, et al. 3D FEM-DEM coupling analysis for ranular-media-based thin-wall elbow tube push-bending process. International Journal of Material Forming. 2019, 12: 985-994

[13] H.D. Hibbit,B.I. Karlsson, P. Sorensen. 2007, Theory Manual, ABAQUS, Version 6.7,

Providence, RI, USA